AD-A090 449 HARRY DIAMOND LABS ADELPHI MD F/G 17/5
THE EXTENSION OF (HG,CD)TE DETECTOR TECHNOLOGY TO THE NEAR-MILL--ETC(U)
JUN 80 B A WEBER, S M KULPA

UNCLASSIFIED NL

1 OF 1
AD A090449

END
DATE FILMED
11-80
DTIC

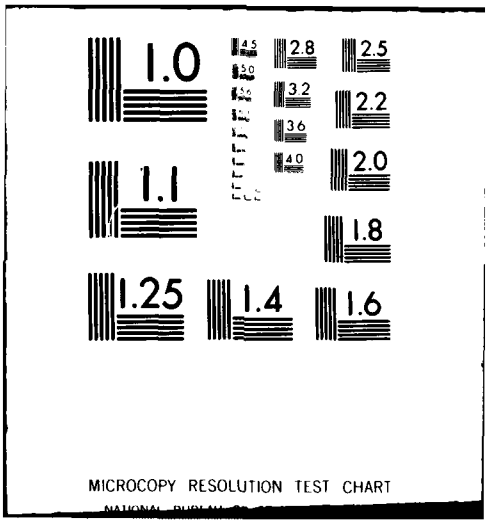
1.0
1.1
1.25
1.4
1.6
1.8
2.0
2.2
2.5
2.8
3.2
3.6
4.0
4.5
5.0
MICROCOPY RESOLUTION TEST CHART

*WEBER and KULPA

THE EXTENSION OF [Hg,Cd]Te DETECTOR TECHNOLOGY TO THE NEAR-MILLIMETER SPECTRAL REGION

BRUCE A. WEBER [redacted] STANLEY M. KULPA, PhD
U.S. ARMY ELECTRONICS RESEARCH AND DEVELOPMENT COMMAND
HARRY DIAMOND LABORATORIES
ADELPHI, MD 20783

JUN 80

This paper discusses

~~We report~~ the development of the first hot-electron photoconductive detector using crystals of the alloy semiconductor mercury-cadmium-telluride, $[Hg_{1-x}, Cd_x]Te$ [1]. When the crystals were irradiated with near-millimeter wave (NMMW) radiation, sensitivity was observed throughout the 100 to 1000 GHz spectral region. These results are significant because they suggest that the extensive [Hg,Cd]Te technology base developed for FLIR systems may also be exploited for the development of NMMW sensors. Such exploitation might lead to the development of hybrid NMMW/IR sensors using only one detection element.

The need for semiconductors with a variable bandgap has led to the study of various ternary compounds. Among these, [Hg,Cd]Te has been developed for use in detectors [2] and lasers [3,4] in the 8 to 14 micrometer spectral region. Operation in the hot-electron photoconductive mode extends the use of this material to the NMMW spectral region. Applications include IR and NMMW heterodyne receivers for all-weather surveillance and tracking systems, NMMW broadband video receivers for spectroscopic studies of materials and atmospheric gases, and submillimeter heterodyne receivers for fusion plasma diagnostics.

BACKGROUND

When radiation is absorbed by a photoconductor, electronic transitions are induced that produce a change in electrical conductivity. This process is distinguishable from bulk thermal effects that raise the temperature of the semiconductor by the fact that the response time of the photoconductive process is usually much shorter than that for the bulk thermal effects.

399

Four types of electronic transitions can lead to photoconductivity. Figure 1 pictorially describes these processes. The upper half shows the electronic transitions while the lower half shows the corresponding spectral response. The four processes are intrinsic, extrinsic, hot-electron (free carrier), and hopping.

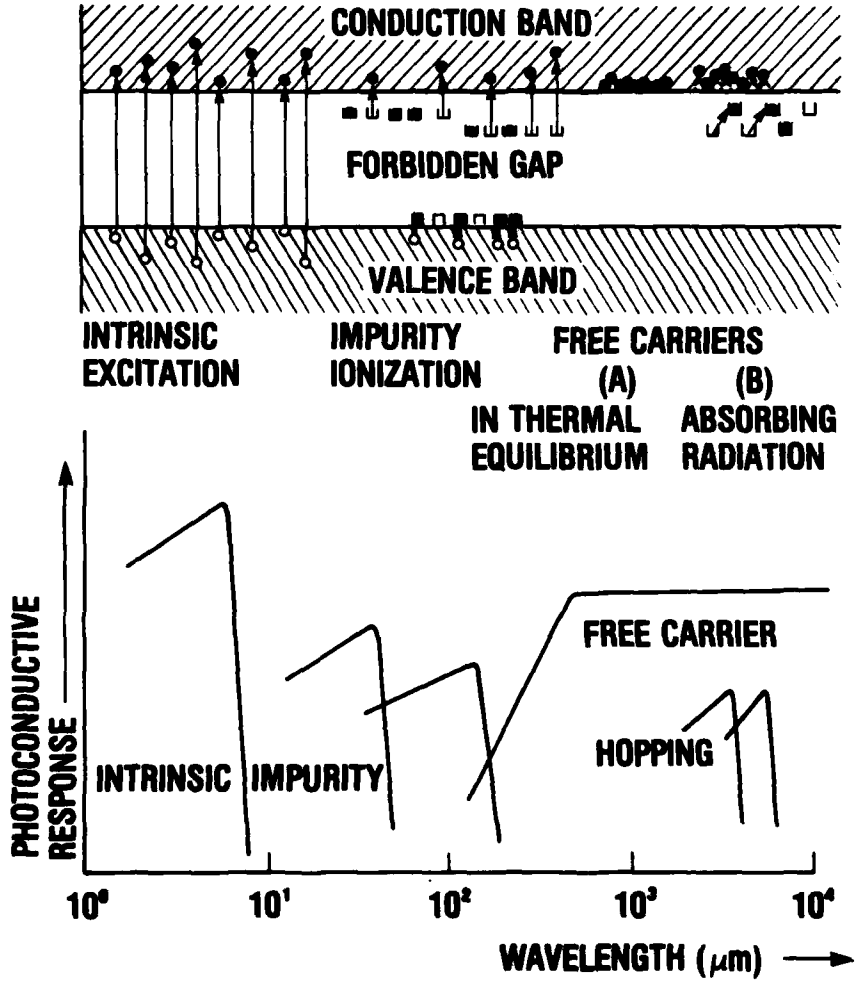

Figure 1. The photoconductive detector. Top half shows electronic transitions. Bottom half shows spectral response.

(400)

Intrinsic photoconductivity arises from electronic transtions between the valence and conduction bands of the semiconductor. Thus the concentration of both free electrons and holes is increased. This process occurs when the photon energy is greater than the energy difference between bands and thus has a long wavelength threshold corresponding to the energy gap. FLIR (8 to 12 μm) system detectors operate via the intrinsic absorption in [Hg,Cd]Te.

At longer wavelengths, impurities can be ionized to provide increased concentrations of electrons or holes. The ionization energy is smaller than the intrinsic energy gap, so that these transitions can be represented as originating at localized states within the gap. The threshold will be at a longer wavelength than the intrinsic threshold, and only one type of free carrier will be produced. This is impurity or extrinsic photoionization.

At still longer wavelengths, hot-electron photoconductivity due to radiation absorption by the free electrons is observed. At low temperatures (≈4 K), the coupling of the electrons to the lattice is much weaker than at room temperature. Thus the electron temperature, which is the same as that of the lattice at room temperature, can be very much different from that of the lattice at low temperatures. This means that radiation absorbed by the electrons can raise the electron temperature above that of the lattice. This increase in electron temperature is observable by a change in the electron mobility and thus the photoconductivity. The process does not have a long wavelength threshold. The absorption, which can be described classically by Drude theory, varies as λ^2 for short wavelengths and becomes constant for wavelengths longer than a characteristic electron-electron interaction length. For NMMW operation the hot-electron mode dominates.

The fourth type of photoconductivity, hopping, is due to electronic tunneling transitions between impurity states. This long wavelength effect is only observed at very low temperatures where freeze-out of free electrons from the conduction band onto impurity sites occurs, thus diminishing the free-electron absorption contribution. Under these conditions, a hopping movement of electrons from donor site to donor site characterizes the observed photoconductivity. This tunneling of donor electrons is due to the small overlap of the electron wave function with that of an adjacent donor site. Thus activation into the conduction band is unnecessary.

Hot-electron photoconductivity in the NMMW spectral region was first observed by Putley [5] using the semiconductor InSb. Rollin [6] has shown that under constant current conditions the absorption is manifest by a change in the free carrier mobility, μ. The

(401)

voltage responsivity, R, is given by

$$R = dV/dP = -(V/\mu)(d\mu/dP),$$

where V is the voltage across the crystal and $d\mu/dP$ is the change in free carrier mobility with incident radiant power, P. Using Kogan's analysis [7] for R with the classical Drude theory of conductivity, it is easy to show that

$$R \propto \alpha \propto (1 + \omega^2\tau_s^2)^{-1} ,$$

where α is the radiation frequency dependent absorption coefficient, ω is the radiation frequency, and τ_s is the electron scattering time. Thus at long wavelengths where $\omega\tau_s << 1$, R will be independent of wavelength, and for short wavelengths were $\omega\tau_s >> 1$, R will vary as λ^2.

EXPERIMENT

Experiments were performed with n-type [Hg,Cd]Te crystals obtained from Cominco American. They were specified to have the IR absorption edge at a wavelength long enough to permit good absorption of CO_2 laser radiation (9 to 11 μm). In addition, the carrier concentration and mobility were selected so as to achieve favorable NMMW detectivity. To date, several samples have operated in the hot-electron photoconductive mode.

Figure 2 is a schematic diagram of the experimental configuration. The $[Hg_{1-x}, Cd_x]Te$ sample used was single crystal n-type with a CdTe mole fraction x of 0.215 ($\lambda_g \simeq 13$ μm at 4 K). Measurements at 77 K indicated a carrier concentration of 7.8×10^{14} cm^{-3} and a mobility of 1.2×10^5 $cm^2/V{\cdot}s$. The 6 x 6 x 0.5 mm sample was etch-polished on the 6 x 6 mm faces, and ohmic contacts were applied to two opposite 6 x 0.5 mm faces by using a high purity indium solder. The detector element was placed in a liquid helium cryostat at the end of a 10 mm diameter, 100 cm long, gold-coated waveguide. A filter was used to attenuate radiation of wavelengths less than 100 μm. The filter consisted of a 2 mm thick clear polyethylene window held at 300 K, a 0.14 mm thick black polyethylene window, and a Z-cut 1 mm thick crystalline quartz window held at 4 K. Radiation entered the circular waveguide from various sources including a 4.3 mm wavelength IMPATT diode, a 2.5 mm wavelength klystron, and optically pumped laser sources at 1.2 mm ($C^{13}H_3F$), 0.496 mm ($C^{12}H_3F$), 0.206 mm (CD_3F), and 0.119 mm (CH_3OH). This radiation was simultaneously monitored with a planar GaAs Schottky barrier diode (SBD) detector and a Scientech calorimeter. The SBD detector was used to monitor signal amplitude variations, while the Scientech calorimeter was used to measure the power entering the [Hg,Cd]Te detector waveguide. Losses due to transmission through the waveguide and filters were accounted for by a

402

separate measurements.

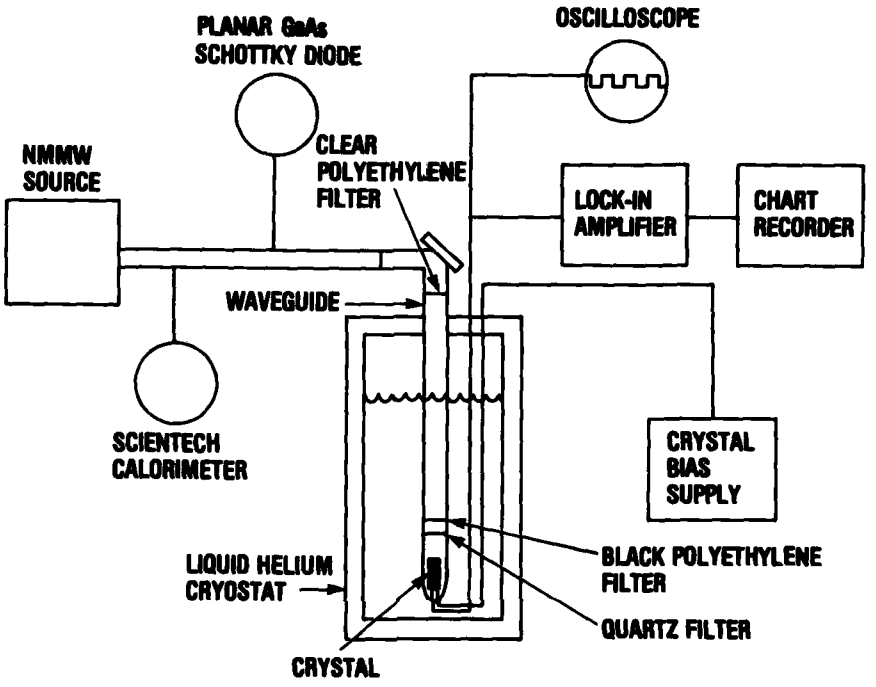

Figure 2. Experimental Configuration

The sensitivity of the detector was measured by using a PAR HR-8 lock-in amplifier with an effective bandwidth of 3 Hz. No other signal amplification was used for the measurements. The temporal response of the detector was measured by pulsing the 2.5 mm wavelength klystron.

RESULTS

Figure 3 shows the relative detector response (λ = 2.5 mm) versus crystal bias current, I_B, for three different incident radiant powers. The three curves yield, in order of increasing power, responsivities of 2.5, 1.3, and 0.9 V/W. The decrease in responsivity by about a factor of 3 is believed to be due to saturation effects.

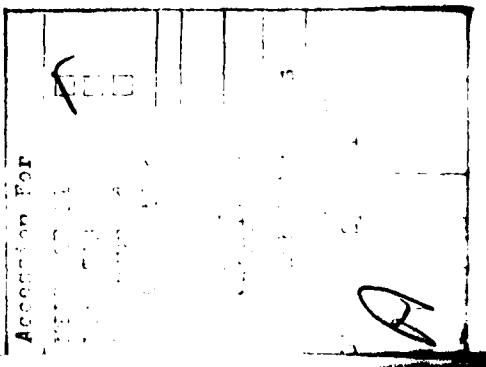

(403)

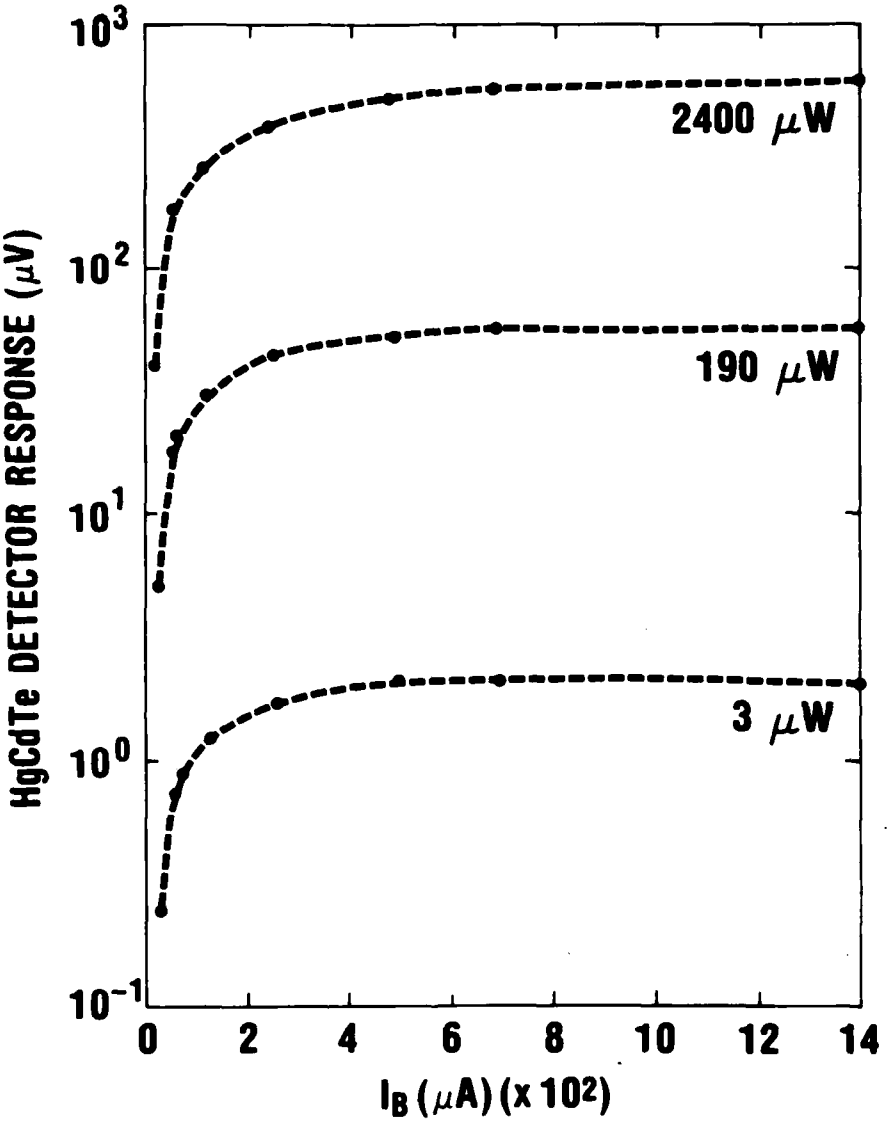

Figure 3. Relative [Hg,Cd]Te detector response at λ = 2.5 mm.

Figure 4 shows the detector spectral responsivity obtained with incident source power averaging approximately 200 μW. A peak responsivity of about 2.5 V/W is observed for wavelengths longer than 1 mm. For shorter wavelengths, the responsivity decreases approxi-

(404)

mately as λ^2, in accordance with the Drude theory. Since the responsivity is proportional to the conductivity, σ, the electron scattering time, τ_s, can be calculated from

$$R = R_{max}/(1 + \omega^2\tau_s^2).$$

From figure 4, $R = R_{max}/2$ when $\lambda = 370$ μm, thus yielding $\tau_s = 2 \times 10^{-13}$s. A calculation using data from Long [8] and $\tau_s = m^*\mu/e$, where m^* is the electron effective mass and μ is the mobility, yields $\tau_s = 5 \times 10^{-13}$ s.

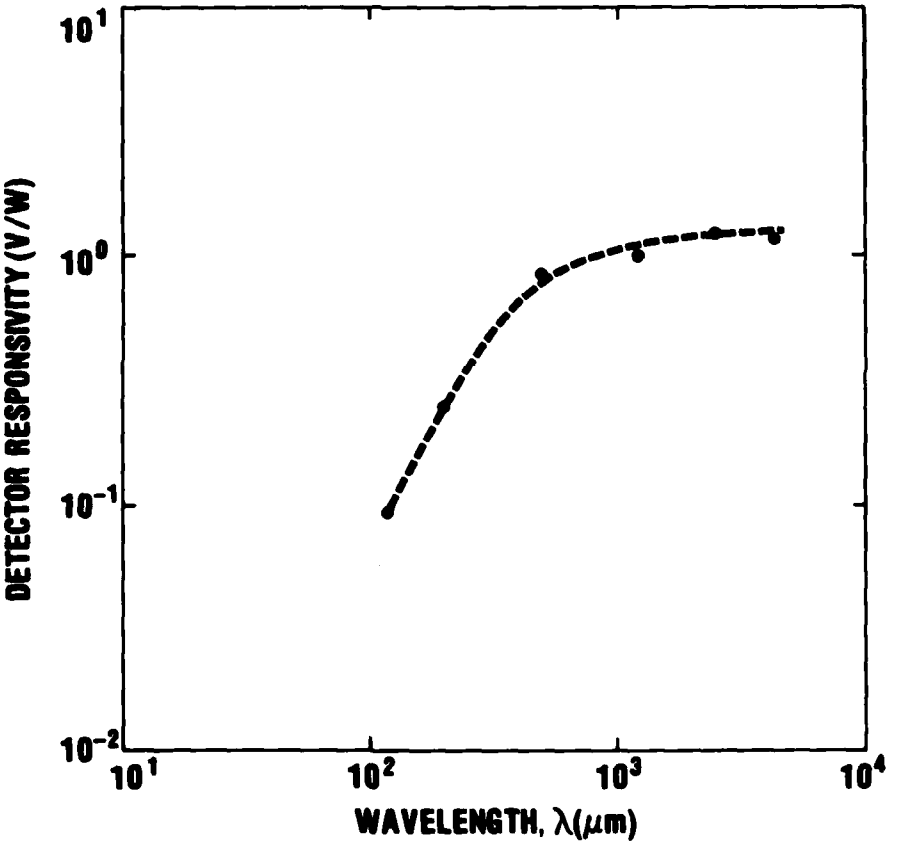

Figure 4. [Hg,Cd]Te spectral response

Figure 5 shows the detector response (λ = 2.5 mm) as a function of the pulse duration. Studies were made with pulse durations varying between 0.1 and 10 μs and rise times of approximately 20 ns. The high speed response rolloff yields an excess carrier lifetime of approximately 300 ns.

405

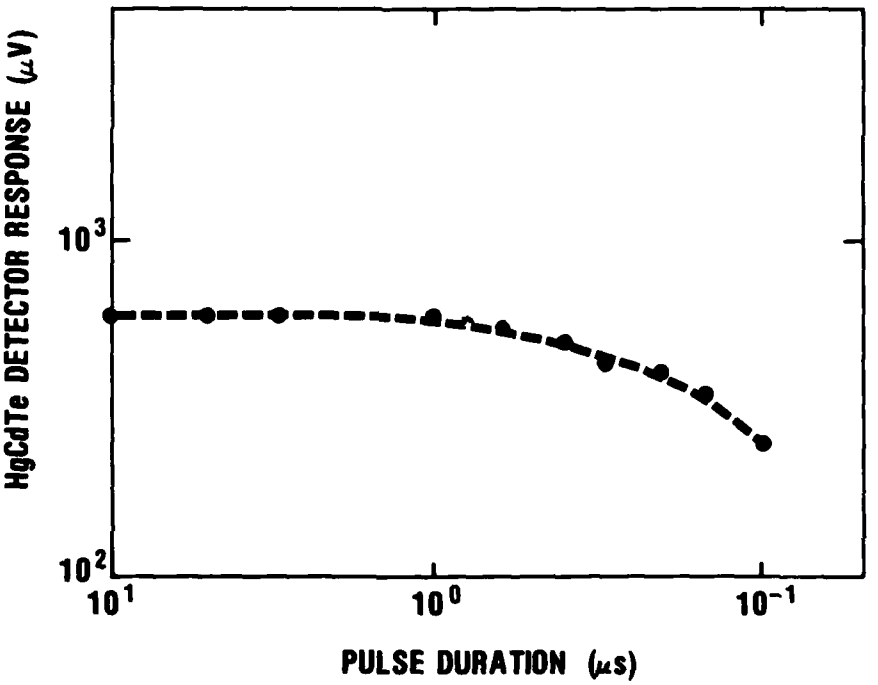

Figure 5. [Hg,Cd]Te temporal response at λ = 2.5 mm.

Figure 6 shows a comparison of the response of a planar GaAs Schottky barrier detector, a Scientech calorimeter, and the hot-electron [Hg,Cd]Te detector to the attenuation of the output of a 2.5 mm wavelength klystron. For an attenuation of up to 30 dBm, the [Hg,Cd]Te detector maintained a nearly linear response.

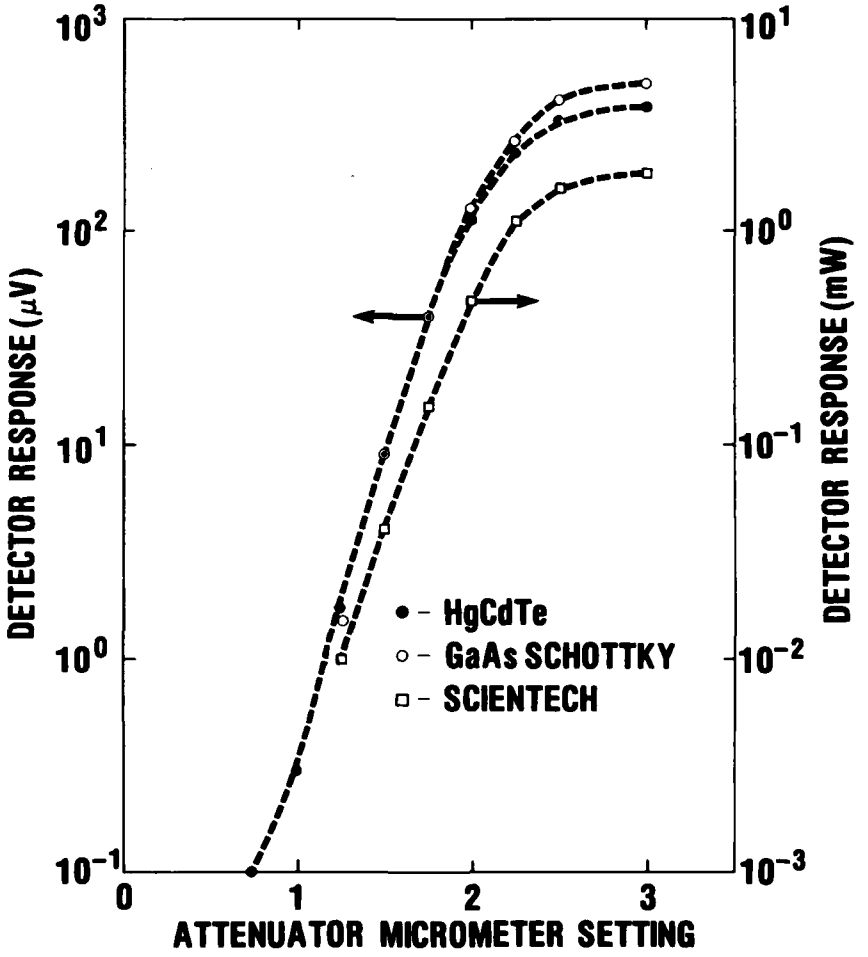

Figure 6. Comparative response of [Hg,Cd]Te detector with Scientech calorimeter and planar GaAs Schottky barrier diode detector.

Operation at 2.5 mm wavelength with optimum system parameters yields a noise equivalent power, NEP, of 2×10^{-10} W/$\sqrt{\text{Hz}}$. A comparative study with a sample of InSb in our dewar in place of the [Hg,Cd]Te crystal yielded an NEP of approximately 1×10^{-10} W/$\sqrt{\text{Hz}}$.

Our reported sensitivity for InSb is nearly a factor of 50 lower than that reported by Kinch and Rollin [9]. This difference is, at least in part, due to a loss in the coupling of the radiation to

the crystal and possibly to differences in crystal parameters (mobility and carrier concentration). Thus it is expected that refinements of coupling geometry and crystal parameters will yield similar improvements in the sensitivity for the [Hg,Cd]Te detector.

SUMMARY

We have observed hot-electron photoconductive detection of NMMW radiation in mercury-cadmium-telluride. Sensitivity is comparable to InSb throughout the NMMW spectral region. The sensitivity rolloff for [Hg,Cd]Te occurs at approximately 600 GHz (0.5 mm) as compared to 300 GHz (1 mm) for InSb, thus extending the useful range of these detectors to considerably shorter wavelengths. It is anticipated that NMMW applications for [Hg,Cd]Te will further the already extensive use of this ternary semiconductor in Army military systems.

REFERENCES

[1] B. A. Weber and S. M. Kulpa, Fourth International Conference on Infrared and Millimeter Waves and Their Applications, Miami Beach, Florida, 148, Dec. 1979.

[2] W. D. Lawson, S. Nielsen, E. H. Putley, and A. S. Young, J. Phys. Chem. Sol., Vol. 9, 325, 1959.

[3] I. Melngailis and A. J. Strauss, Appl. Phys. Lett., Vol 8, 179, 1966.

[4] B. A. Weber, J. P. Sattler, and J. Nemarich, Appl. Phys. Lett., Vol. 27, 93, 1975.

[5] E. H. Putley, J. Phys. Chem., Vol. 22, 241, 1961.

[6] B. V. Rollin, Proc. Phys. Soc. Cond., Vol. 77, 1102, 1961.

[7] S. M. Kogan, Sov. Phys. Sol. St., Vol. 4, 1812, 1963.

[8] D. Long, Phys. Rev., Vol. 176, 923, 1968.

[9] M. A. Kinch and R. V. Rollin, Brit. J. Appl. Phys., Vol. 14, 672, 1963.


DAT
FILM